Cucurbit[8]uril-Regulated Nanopatterning of Binary Polymer Brushes via Colloidal Templating

*Chi Hu, Yang Lan, Kevin R. West, and Oren A. Scherman**

Interest in the fabrication of micro-/nanopatterned polymer surfaces with high precision has grown substantially in recent years, on account of potential applications in surface-based technologies including photovoltaic devices,[1] semiconductors,[2,3] photonic crystals,[4] nanofluidic devices,[5] and platforms for tissue engineering.[6] In particular, development of less stringent alternative approaches to traditional nanoimprint lithography methods, which use photons or electrons to modify the chemical and physical properties of surface-bound resins, is crucial in many areas, for example, photonics, chip-based sensors, and most biological applications.[7] Polymer brushes are widely applied in surface engineering as alternatives to self-assembled monolayers due to their mechanical and chemical robustness, coupled with a high degree of synthetic flexibility and facile incorporation of functional moieties.[8] Patterned polymer brushes have attracted considerable interest not only in a myriad of applications, ranging from semiconductors[9] to biomaterials,[10] but also as useful tools to study fundamental questions of surface-tethered polymer films, such as swelling behavior or molecular organization.[11,12] Despite numerous strategies such as microcontact printing,[13] electron beam,[14] or UV irradiation[15] assisted nanolithography techniques for both laboratory and industrial use to prepare patterned polymer surfaces, few approaches have been reported for the preparation of laterally patterned binary brushes on the sub-micrometer scale under ambient conditions.[16,17]

The monolayer colloidal crystal (MCC) templated self-assembly process has proven to be a promising alternative strategy to fabricate ordered arrays with well-defined micro and nanostructures because of its flexibility and controllable morphologies.[18–21] Since Deckman et al. reported the formation of identical sub-micrometer microcolumnar structures in 1982,[22] the MCC templating approach has been employed to prepare various ordered micro-/nanostructures such as nanosphere arrays,[23] nanoring arrays,[24] and hierarchical polymer surfaces,[25] by different methods including dip coating,[26] spin coating,[27] electrochemical deposition,[28] etc. A main challenge that remains in the area of MCC templating is the controllable and reversible immobilization of colloidal particles on surfaces.[29] For example, in the fabrication of hierarchical binary structures, the surface-attachment should be strong enough so the colloids do not fall off the surface during the assembly of the first required material, yet need to be easily removed from the surface on demand to leave void spaces available for subsequent material deposition.[30,31]

We herein demonstrate a solely supramolecular route as a promising alternative process for the preparation of sub-micrometer and nanopatterned brush surfaces. Cucurbit[8]uril (CB[8]) is a pumpkin-shaped macrocyclic host that has received tremendous interest in the supramolecular community, on account of its ability to simultaneously incorporate two guest molecules (e.g., viologen (MV^{2+}) as the first guest and azobenzene (Azo) or naphthol (Np) as the second guest) and their exceptional recognition properties in aqueous medium.[32–35] Recently, our group reported a CB[8]-based rotaxane structure on Au surfaces, where CB[8] is threaded onto a MV^{2+} core and prevented from dissociation away from the surfaces. The reversible formation of colloidal monolayers on Au surfaces through the host–guest interaction between these surface-bound CB[8] rotaxanes and Azo functionalized silica microspheres (Azo-Si) was also described.[36,37] We now further explore the application of these supramolecularly assembled colloidal monolayers in the MCC templated formation of sub-micrometer and nanopatterned polymer brushes.

The four-step protocol for the patterning of binary brush surfaces is illustrated in **Figure 1**. First, a *trans*-Azo-Si colloidal crystal monolayer was assembled on a CB[8]-rotaxane functionalized Au surface using a dip coating technique, which allows the monolayer deposition of particles in hexagonal arrangement on the substrate (Figure 1A). The Azo-Si colloids were prepared by postmodification of bare silica microspheres with 4-hydroxyazobenzene-functionalized silane with a hydrodynamic diameter of 455 nm (polydispersity, PD = 0.046) as measured by dynamic light scattering (see Figure S1B in the Supporting Information). The ordered hexagonal arrangement of Azo-Si on the surface was verified by both scanning electron microscopy (SEM) and atomic force microscopy (AFM) (**Figure 2**), which showed a diameter of 333 nm for the particles. This MCC serves as a template in the next step for the supramolecular assembly of the first polymer, a naphthol functionalized poly(ethylene glycol) (M_n = 2000 g mol^{-1}, Np-PEG$_{2k}$), on the surface.

In the second step, as illustrated in Figure 1B, Np-PEG$_{2k}$ was used to fill in the interstitial vacancies between the Azo-Si colloids leading to polymer brush structures through the formation of heteroternary complexes (Np-PEG·MV^{2+}) ⊂ CB[8]

C. Hu, Dr. Y. Lan, Prof. O. A. Scherman
Melville Laboratory for Polymer Synthesis
Department of Chemistry
University of Cambridge
Cambridge CB2 1EW, UK
E-mail: oas23@cam.ac.uk
Dr. K. R. West
BP Oil UK Ltd
Whitchurch Hill, Pangbourne, Reading
Berkshire RG8 7QR, UK

DOI: 10.1002/adma.201503844

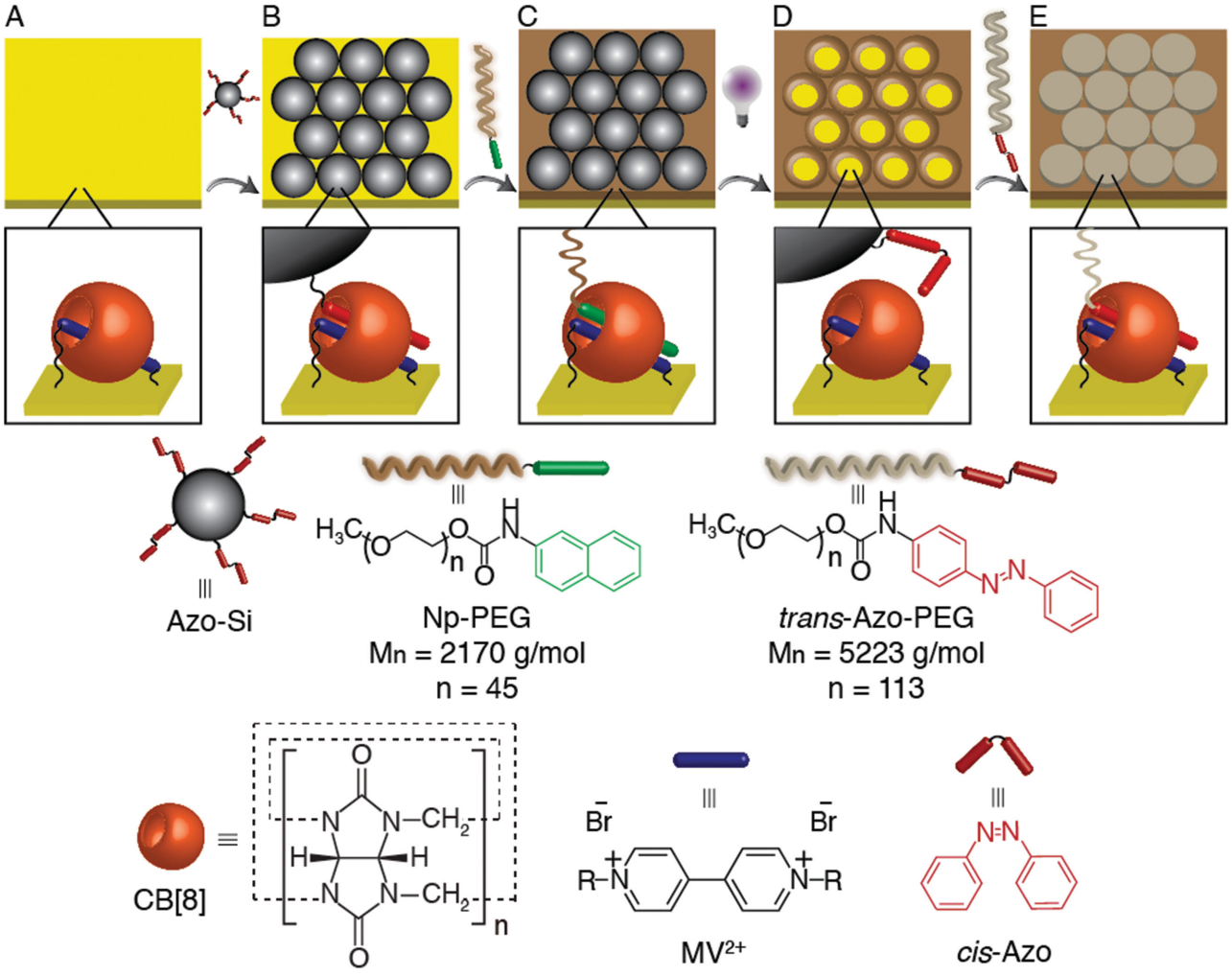

Figure 1. Stepwise preparation of nanopatterned dual polymer brushes via the reversible host–guest complexation of CB[8]. A) Assembly of Azo-Si colloids on the CB[8]-rotaxane functionalized surface through the heteroternary complex formation of (*trans*-Azo·MV^{2+})⊂CB[8]. B) Preparation of Np-PEG_{2k} brushes on the void spaces around Azo-Si colloids on the surface via the incorporation of Np functionalities into the CB[8]-rotaxane cavities. C) Removal of the Azo-Si colloids from the surface by applying UV light (350 nm, 1 min), with the *trans*-Azo photoisomerized to *cis*-Azo and be expelled out of the CB[8] cavity. D) Grafting of the Azo-PEG_{5k} brushes on the empty spaces vacated by Azo-Si colloids.

at the interface, using methodology previously demonstrated by our group.[38] The SEM and AFM topography images do not exhibit much difference before (Figure 2) or after (**Figure 3**) the grafting of Np-PEG_{2k} brushes, because the Azo-Si particles are much larger compared to the height of the Np-PEG brushes. The advantage of using the supramolecular chemistry to attach brushes on the surface in a "grafting to" fashion is its ability to carry out the brush assembly in ambient conditions without the requirement of further chemical reactions and any special instruments, e.g., cyclic voltammetry (CV) for electropolymerization.

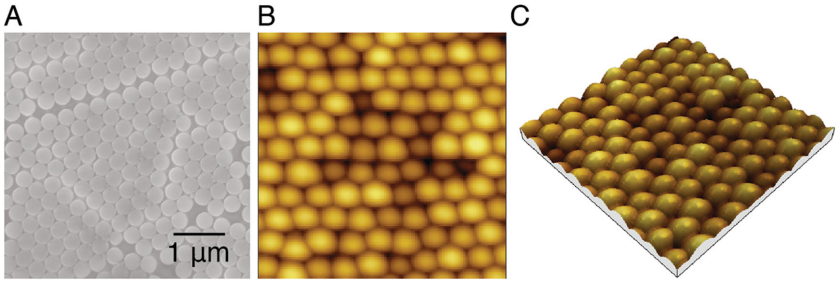

Figure 2. Microscopy images of the Azo-Si monolayer colloidal crystal. A) SEM image, B) AFM 2D topography image (3 μm × 3 μm), and C) AFM 3D topography image (3 μm × 3 μm).

The high hexagonal ordering of the colloidal particles on the surface was well-preserved after the assembly of Np-PEG_{2k} brushes (Figure 3); the assembly process involves the immersion of the substrate in an aqueous solution of Np-PEG_{2k} (5×10^{-3} M) for 30 min on a shaker (200 rpm). Note, this robust immobilization of the Azo-Si colloids to the surface is only made possible by employing the CB[8]-mediated host–guest interaction at the interface to "stick" the particles onto the surface. In an analogous control

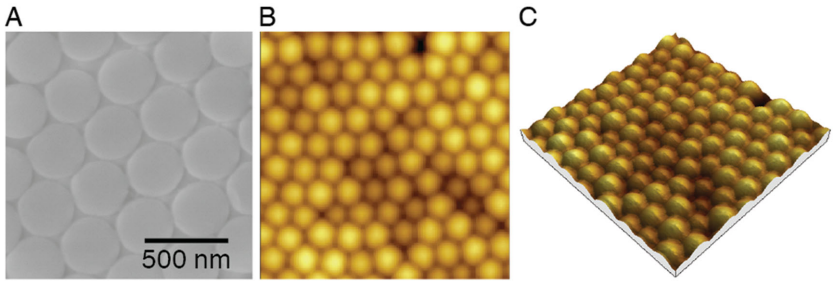

Figure 3. Microscopy images showing the ordered monolayer Azo-Si particles with their gaps filled with Np-PEG_{2k} brushes. A) SEM image, B) AFM 2D topography image (3 μm × 3 μm), and C) AFM 3D topography image (3 μm × 3 μm).

experiment where Azo-Si colloids were dip coated on an unfunctionalized Au substrate, the Azo-Si particles fell off the surface during the assembly process of the Np-PEG_{2k} brushes as water washes off the particles and destroys the ordering. It is noteworthy that although Np exhibits a higher binding constant (6.1×10^5 M^{-1}) to $MV^{2+} \subset$ CB[8] than Azo derivatives (1.4×10^4 M^{-1}), the MCC structure of the Azo-Si microspheres was well-maintained during the assembly of Np-PEG_{2k} brushes. This is likely on account of the multivalent nature of the binding between the Azo-Si colloids and the CB[8]-functionalized substrate.[33,34,39]

In the third step (see Figure 1C), the Azo-Si particles were removed from the surface to expose a dotted pattern with "free" surface-bound CB[8]-rotaxanes, capable of further complexation with second guests. The Azo-Si colloids serve as a sacrificial template for the preparation of ordered Np-PEG_{2k} brushes and their controlled removal was achieved by the *trans*-to-*cis* isomerization of the Azo functionalities on the periphery of the particle surfaces upon UV light irradiation (350 nm, 1 min). While the *trans*-Azo can be incorporated into the CB[8]-rotaxane structure via heteroternary complex formation and "stick" the Azo-Si colloids onto the surface, the *cis*-Azo will dissociate from the CB[8] cavity, resulting in the release of the Azo-Si colloids from the surface. SEM analysis (**Figure 4**A) confirmed that the Np-PEG_{2k} brushes were retained as a monolayer array on the surface and self-assembled not only in-between but also at the interstitial void spaces underneath the Azo-Si. As shown in Figure 4B,C, AFM topography measurements of the ordered Np-PEG_{2k} network depict a periodical cavity of 333 nm in diameter, which matches the size of the Azo-Si colloidal template. The AFM line profile as shown in Figure 4D reported an average height of the cavity equivalent to 10 nm. Surfaces modified with ethylene glycol units have shown to resist nonspecific adsorption of proteins and cells, thus may find potential applications as biomedical coatings.[40–43]

In order to prepare ordered dual polymer brushes, as schematically illustrated in Figure 1D, the cavities created by removing the Azo-Si colloids were back-filled with a second polymer Azo-PEG_{5k}. Azo-PEG_{5k} is a poly(ethylene glycol) (M_n = 5000 g mol^{-1}) end-functionalized with an azobenzene group. A longer PEG chain was used in Azo-PEG_{5k} compared to Np-PEG_{2k} to provide a contrast in heights between the two polymer brushes, in order to obtain a visible pattern. After immersing the substrate in a solution of Azo-PEG_{5k} (5×10^{-3} M) for 30 min on a shaker (200 rpm), the adsorption of the Azo-PEG_{5k} brushes into the cavities via CB[8]-directed heteroternary complex formation can be clearly seen. As shown by the SEM and AFM topography images in **Figure 5**A–C, the periodical patterning is well-maintained after the assembly of the second polymer Azo-PEG_{5k}. An average increase of ≈30 nm in height of the inside cavities after grafting Azo-PEG_{5k} brushes was determined in the line profile obtained from a zoomed-in scan with AFM (see Figure 5D,F).

Force-distance curves of Np-PEG_{2k} and Azo-PEG_{5k} were recorded by approaching a bare Si_3N_4 AFM tip to different areas of the surface (Figure 5D), to further confirm the existence of dual polymer brushes on the surface and their difference in terms of brush height. The brown force spectroscopy curve in Figure 5E was taken on the dark area and exhibited a brush height of 9 nm for the Np-PEG_{2k} brushes, while the yellow curve was obtained on the bright area and resulted in a thickness of 26 nm for the Azo-PEG_{5k} brushes. Note that the slight inconsistency in brush height between AFM topography and force spectroscopy is due to the fact that the topography images were taken in tapping mode, while the force–distance curves were measured in contact mode.

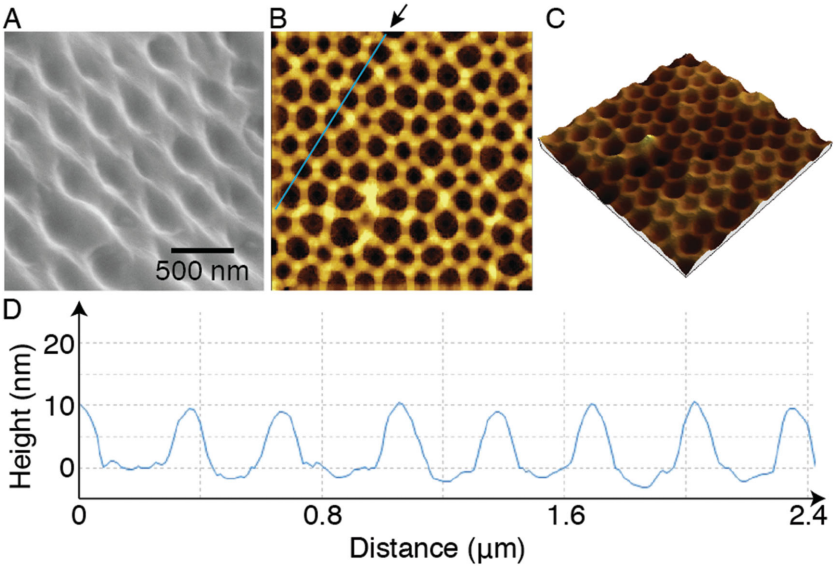

Figure 4. Microscopy images showing the inverse pattern of Np-PEG_{2k} brushes after the removal of Azo-Si colloids. A) SEM image, B) AFM 2D topography image (3 μm × 3 μm), and C) AFM 3D topography image (3 μm × 3 μm). D) The line profile taken along the blue line as indicated by arrow in (B).

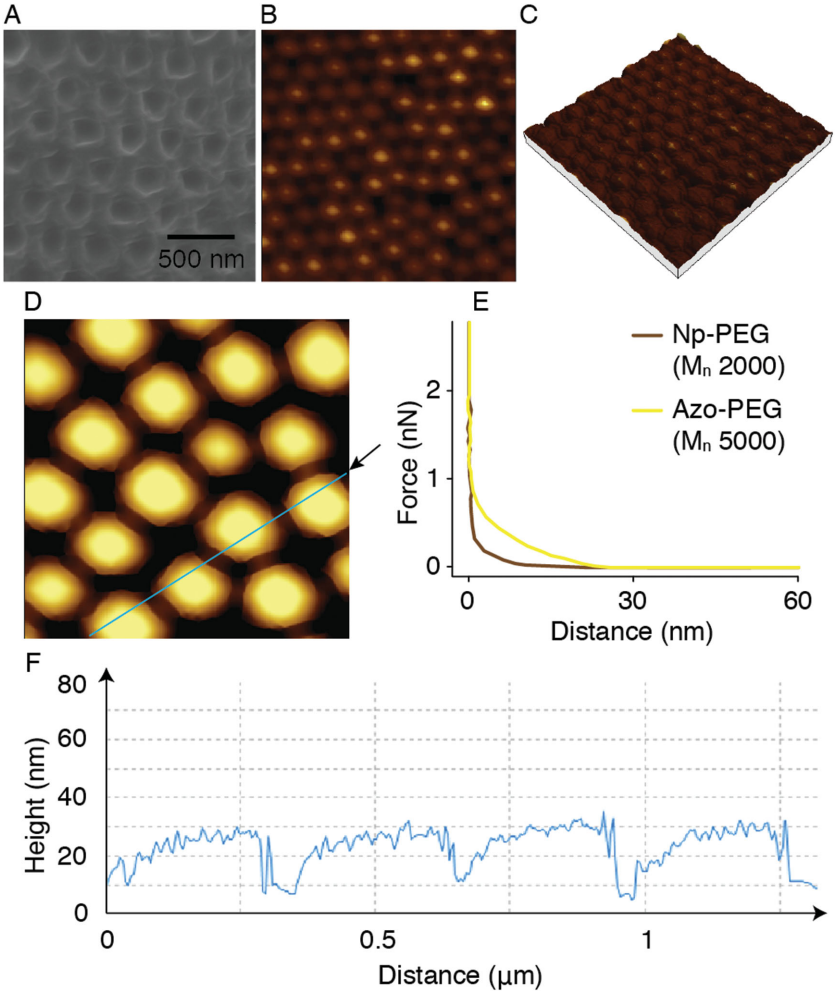

Figure 5. Nanopatterned dual brushes of Np-PEG$_{2k}$ and Azo-PEG$_{5k}$. A) SEM image, B) low-magnification AFM 2D topography image (3 μm × 3 μm) and C) AFM 3D topography image (3 μm × 3 μm) of the dual brushes. D) High-magnification AFM 2D topography image (1.3 μm × 1.3 μm). E) Approach force–distance curves of the Np-PEG$_{2k}$ brushes (brown line, taken on the dark areas in (D)) and the Azo-PEG$_{5k}$ brushes (yellow line, taken on the bright areas in (D)) on the dual brush pattern. F) The line profile taken along the blue line as indicated by arrow in (B).

CV was employed to evaluate the accessible area (A_{sur}) of the modified gold substrates at the different stages of the self-assembly process outlined in Figure 1 of the binary polymer brushes. **Figure 6** shows typical voltammograms for the $Fe(CN)_6^{3-}$/$Fe(CN)_6^{4-}$ oxidation at the modified gold electrode. The CB[8]-functionalized gold electrode is redox-responsive as indicated by the black curve in Figure 6, the current (i_p) decreased from 90 to 31 μA (a reduction of 66%) after assembly of the Azo-Si colloids on the electrode (blue curve).[45] As i_p is directly proportional to A_{sur} under constant scan rate, this significant decrease in i_p can be attributed to the fact that the well-ordered Azo-Si colloidal crystal blocks the electron-transfer event thereby reducing A_{sur}.[46] A further decrease in i_p to only 3 μA (90% overall decrease in current) was observed (red curve) after the assembly of Np-PEG$_{2k}$ brushes; the electrochemically inactive PEG polymer brushes cover the remaining, accessible gold surface, further reducing A_{sur}. The removal of Azo-Si colloids by UV light irradiation exposed spherically patterned CB[8]-functionalized surfaces causing an increase in A_{sur} and resulting in a boost in i_p to 39 μA (a 12-fold increase in current, brown curve). Finally, a gold electrode modified with patterned binary polymer brushes containing both Np-PEG$_{2k}$ and Azo-PEG$_{5k}$ exhibited a negligible i_p (green curve), as the dense layer of polymer brushes rendered the gold electrode completely insulating and stopped the flow of electrons to the surface.

In this stepwise approach to prepare nanopatterned dual polymer brushes, the changes in the composition of

Importantly, the patterned supramolecular Np-PEG$_{2k}$ brushes (Figure 1D) remained stable on the CB[8]-functionalized surface during the subsequent assembly of the longer Azo-PEG$_{5k}$ brushes. Previously, we have shown that Np-PEG brushes did not exhibit any significant decrease in height after 5 h of continuous washing with an aqueous solution of a small molecule Np derivative ([Np] = 1×10^{-3} M).[38] Here, the stability of the Np-PEG$_{2k}$ brushes in the presence of a solution of Azo-PEG$_{5k}$ is even greater as the likelihood of competitive surface displacement with end-functionalized Azo-PEG$_{5k}$ "polymer chains" is substantially lower. The observed robust nature of the supramolecular PEG brushes is likely due to a multivalent "carpet effect" created by the presence of multiple H_2O bridges exploiting hydrogen bonds between oxygen atoms of neighboring PEG chains.[44] These H_2O bridges are only possible when the distance between two adjacent PEG polymer chains is necessarily low.

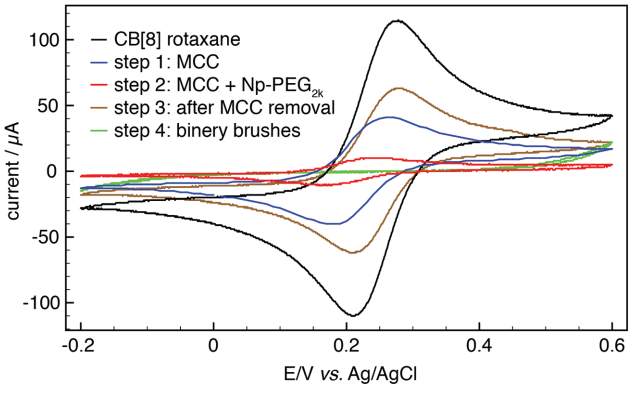

Figure 6. Cyclic voltammograms of $Fe(CN)_6^{3-}$/$Fe(CN)_6^{4-}$ (0.5×10^{-3} M) in 0.5 M KCl solution obtained using the modified gold substrate as the working electrode, a silver chloride electrode as the reference electrode. Scans start from –0.2 to 0.6 V, with a scan rate of 50 mV s^{-1}.

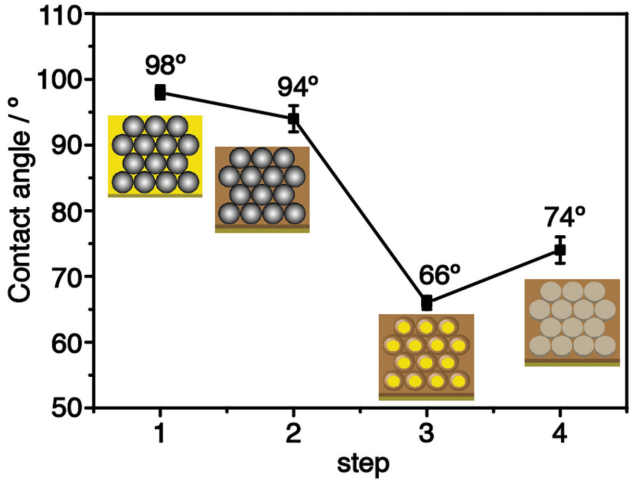

Figure 7. Water contact angle measurements for the four stages in the stepwise preparation of nanopatterned dual polymer brushes.

surface-bound materials can also be followed by water contact angle measurements. As shown in **Figure 7**, a contact angle (CA) of 98° was measured on the substrate with hexagonally ordered Azo-Si colloids. After filling the gaps with Np-PEG_{2k} on the surface, the CA decreased slightly to 94°. The CA was further reduced to 66° after removal of Azo-Si colloids with UV irradiation. Note that this value is higher than the CA for both the CB[8]-rotaxane functionalized surface (43°) and the homogeneous Np-PEG_{2k} brush-modified surface (61°).[38] The CA increased to 74° after back-filling the void spaces on the surface vacated by the Azo-Si spheres, and again this value is higher than the CA for either the Np-PEG_{2k} brushes (61°) or Azo-PEG_{5k} (61°) brushes grafted to the surface. This slight increase in hydrophobicity (61° to 74°) is likely because the nanopatterned structures on the surface make it more hydrophobic.[47] The observed phenomena that the nanopatterned dual-composite structures made the surface more hydrophobic than surfaces modified with either of the individual components opens up opportunities to fabricate superhydrophobic surfaces using our supramolecular assembly strategy.

In conclusion, we have developed a facile and lithography-free approach to creating topologically and chemically defined polymer surfaces under mild and ambient conditions by combining the techniques of MCC-templated patterning, host–guest complexation and orthogonally controlled supramolecular self-assembly. Dual composition nanopatterned brushes have been prepared by employing CB[8]-rotaxanes as supramolecular linking agents on gold surfaces to controllably "stick" *trans*-Azo functionalized silica colloids onto the surface in a hexagonal arrangement, which serve as a template for the assembly of short polymer brushes. The formed MCC is photoresponsive and can be reversibly disassembled upon UV light irradiation to create void spaces for the grafting of a second, longer polymer brush to form a dual pattern on the nanoscale. To the best of our knowledge, this is the first example of host–guest recognition directed sub-micrometer nanopatterning of binary brushes using MCC as a template. This facile supramolecular approach provides a platform to prepare nanopatterned composite brushes with sophisticated structures under mild conditions, and may prove useful in a number of potential applications including dual responsive sensor films and biomedical coatings.

Supporting Information

Supporting Information is available from the Wiley Online Library or from the author.

Acknowledgements

This work was supported by the Engineering Physical Science Research Council, grant EP/K028510/1; C.H. thanks BP for financial support and Y.L. is grateful for a CSC Cambridge Scholarship.

Received: April 19, 2015
Revised: May 13, 2015
Published online: October 28, 2015

[1] X. He, F. Gao, G. Tu, D. Hasko, S. Hüttner, U. Steiner, N. C. Greenham, R. H. Friend, W. T. S. Huck, *Nano Lett.* **2010**, *10*, 1302.
[2] E. Menard, M. A. Meitl, Y. Sun, J.-U. Park, D. J.-L. Shir, Y.-S. Nam, S. Jeon, J. A. Rogers, *Chem. Rev.* **2007**, *107*, 1117.
[3] O. Fenwick, L. Bozec, D. Credgington, A. Hammiche, G. M. Lazzerini, Y. R. Silberberg, F. Cacialli, *Nat. Nanotechnol.* **2009**, *4*, 664.
[4] Z. Nie, E. Kumacheva, *Nat. Mater.* **2008**, *7*, 277.
[5] R. Y. H. Lim, J. Deng, *ACS Nano* **2009**, *3*, 2911.
[6] E. K. F. Yim, R. M. Reano, S. W. Pang, A. F. Yee, C. S. Chen, K. W. Leong, *Biomaterials* **2005**, *26*, 5405.
[7] L. J. Guo, *Adv. Mater.* **2007**, *19*, 495.
[8] S. Edmondson, V. L. Osborne, W. T. S. Huck, *Chem. Soc. Rev.* **2004**, *33*, 14.
[9] R. Barbey, L. Lavanant, D. Paripovic, N. Schüwer, C. Sugnaux, S. Tugulu, H.-A. Klok, *Chem. Rev.* **2009**, *109*, 5437.
[10] R. Iwata, P. Suk-In, V. P. Hoven, A. Takahara, K. Akiyoshi, Y. Iwasaki, *Biomacromolecules* **2004**, *5*, 2308.
[11] M. Husemann, M. Morrison, D. Benoit, J. Frommer, C. M. Mate, W. D. Hinsberg, J. L. Hedrick, C. J. Hawker, *J. Am. Chem. Soc.* **2000**, *122*, 1844.
[12] R. R. Shah, D. Merreceyes, M. Husemann, I. Rees, N. L. Abbott, C. J. Hawker, J. L. Hedrick, *Macromolecules* **2000**, *33*, 597.
[13] B. Zhao, W. J. Brittain, *Prog. Polym. Sci.* **2000**, *25*, 677.
[14] S. J. Ahn, M. Kaholek, W.-K. Lee, B. LaMattina, T. H. LaBean, S. Zauscher, *Adv. Mater.* **2004**, *16*, 2141.
[15] L. Ionov, S. Minko, M. Stamm, J.-F. Gohy, R. Jérôme, A. Scholl, *J. Am. Chem. Soc.* **2003**, *125*, 8302.
[16] Y. Liu, V. Klep, I. Luzinov, *J. Am. Chem. Soc.* **2006**, *128*, 8106.
[17] R. B. Pernites, E. L. Foster, M. J. L. Felipe, M. Robinson, R. C. Advincula, *Adv. Mater.* **2011**, *23*, 1287.
[18] Z. L. Wang, *Adv. Mater.* **1998**, *10*, 13.
[19] X. D. Wang, E. Graugnard, J. S. King, Z. L. Wang, C. J. Summers, *Nano Lett.* **2004**, *4*, 2223.
[20] S.-M. Yang, S. G. Jang, D.-G. Choi, S. Kim, H. K. Yu, *Small* **2006**, *2*, 458.
[21] C. L. Haynes, R. P. Van Duyne, *J. Phys. Chem. B* **2001**, *105*, 5599.
[22] H. W. Deckman, J. H. Dunsmuir, *Appl. Phys. Lett.* **1982**, *41*, 377.
[23] X. Ye, L. Qi, *Nano Today* **2011**, *6*, 608.
[24] F. Sun, J. C. Yu, X. Wang, *Chem. Mater.* **2006**, *18*, 3774.
[25] P. Jiang, M. J. McFarland, *J. Am. Chem. Soc.* **2004**, *126*, 13778.

[26] A. S. Dimitrov, K. Nagayama, *Langmuir* **1996**, *12*, 1303.
[27] G. A. Ozin, S. M. Yang, *Adv. Funct. Mater.* **2001**, *11*, 95.
[28] F. Sun, W. P. Cai, Y. Li, B. Cao, F. Lu, G. Duan, L. Zhang, *Adv. Mater.* **2004**, *16*, 1116.
[29] O. D. Velev, A. M. Lenhoff, *Curr. Opin. Colloid In.* **2000**, *5*, 56.
[30] C. A. Nijhuis, J. Huskens, D. N. Reinhoudt, *J. Am. Chem. Soc.* **2004**, *126*, 12266.
[31] O. Crespo-Biel, B. Dordi, D. N. Reinhoudt, J. Huskens, *J. Am. Chem. Soc.* **2005**, *127*, 7594.
[32] D. Das, O. A. Scherman, *Israel J. Chem.* **2011**, *51*, 537.
[33] E. A. Appel, F. Biedermann, U. Rauwald, S. T. Jones, J. M. Zayed, O. A. Scherman, *J. Am. Chem. Soc.* **2010**, *132*, 14251.
[34] F. Tian, D. Jiao, F. Biedermann, O. A. Scherman, *Nat. Commun.* **2012**, *3*, 1207.
[35] H. Yang, B. Yuan, X. Zhang, O. A. Scherman, *Acc. Chem. Res.* **2014**, *47*, 2106.
[36] C. Hu, Y. Lan, F. Tian, K. R. West, O. A. Scherman, *Langmuir* **2014**, *30*, 10926.
[37] C. Hu, Y. Zheng, Z. Yu, C. Abell, O. A. Scherman, *Chem. Commun.* **2015**, *51*, 4858.
[38] C. Hu, F. Tian, Y. Zheng, C. Soo, Y. Tan, K. R. West, O. A. Scherman, *Chem. Sci.* **2015**, *6*, 5303.
[39] U. Rauwald, F. Biedermann, S. Deroo, C. V. Robinson, O. A. Scherman, *J. Phys. Chem. B* **2010**, *114*, 8606.
[40] P. Harder, M. Grunze, R. Dahint, G. M. Whitesides, P. E. Laibinis, *J. Phys. Chem. B* **1998**, *102*, 426.
[41] K. L. Prime, G. M. Whitesides, *Science* **1991**, *252*, 1164.
[42] H. Ma, J. Hyun, P. Stiller, A. Chilkoti, *Adv. Mater.* **2004**, *16*, 338.
[43] L. G. Harris, S. Tosatti, M. Wieland, M. Textor, R. G. Richards, *Biomaterials* **2004**, *25*, 4135.
[44] R. L. C. Wang, H. J. Kreuzer, M. Grunze, *J. Phys. Chem. B* **1997**, *101*, 9767.
[45] F. Tian, M. Cziferszky, D. Jiao, K. Wahlström, J. Geng, O. A. Scherman, *Langmuir* **2011**, *27*, 1387.
[46] A. L. Eckermann, D. J. Feld, J. A. Shaw, T. J. Meade, *Coord. Chem. Rev.* **2010**, *254*, 1769.
[47] Y. C. Jung, B. Bhushan, *Nanotechnology* **2006**, *17*, 4970.